

Novel allosteric glutaminase 1 inhibitors with macrocyclic structure activity relationship analysis

Eun Ji Lee^{a,1}, Krishna Babu Duggirala^{b,c,1}, Yujin Lee^{b,c,1}, Mi Ran Yun^{d,e,1}, Jiyeon Jang^{b,f}, Rajath Cyriac^{b,c}, Myoung Eun Jung^b, Gildon Choi^{b,c}, Chong Hak Chae^b, Byoung Chul Cho^{g,*}, Kwangho Lee^{b,c,*}

^a Department of Research Support, Yonsei Biomedical Science Institute, Yonsei University College of Medicine, Seoul 03722, South Korea

^b Bio & Drug Discovery Division, Korea Research Institute of Chemical Technology, Daejeon 34114, South Korea

^c Medicinal Chemistry & Pharmacology, University of Science & Technology, Daejeon 34113, South Korea

^d Severance Biomedical Science Institute, Yonsei University College of Medicine, Seoul 03722, South Korea

^e Yonsei New Li Han Institute for Integrative Lung Cancer Research, Yonsei University College of Medicine, Seoul 03722, South Korea

^f Department of Chemistry, Sungkyunkwan University, Suwon 16419, South Korea

^g Division of Medical Oncology, Department of Internal Medicine, Yonsei Cancer Center, Yonsei University College of Medicine, Seoul 03722, South Korea

ARTICLE INFO

Dedicated to Professor Jin K. Cha on the occasion of his 70th birthday.

Keywords:

Glutaminase 1
GLS1
Macrocyclic
Anticancer
KRAS
KEAP1
BPTES
Cancer metabolism

ABSTRACT

Glutamine-addicted cancer metabolism is recently recognized as novel cancer target especially for KRAS and KEAP1 co-occurring mutations. Selective glutaminase1 (GLS1) inhibition was reported using BPTES which has novel mode of *allosteric* inhibition. However, BPTES is a highly hydrophobic and symmetric molecule with very poor solubility which results in suboptimal pharmacokinetic parameters and hinders its further development. As an ongoing effort to identify more drug-like GLS1 inhibitors via systematic *structure – activity relationship* (SAR) analysis of BPTES analogs, we disclose our novel macrocycles for GLS1 inhibition with conclusive SAR analysis on the core, core linker, and wing linker, respectively. Selected molecules resulted in reduction in intracellular glutamate levels in LR (LDK378-resistant) cells which is consistent to cell viability result. Finally, compounds 13 selectively reduced the growth of A549 and H460 cells which have co-occurring mutations including KRAS and KEAP1.

Normally differentiated cells rely primarily on mitochondrial oxidative phosphorylation to generate the energy required for cellular processes. However, most cancer cells develop extensive reprogramming of cellular energy metabolism and rely on modified aerobic glycolysis, named the “Warburg effect”.¹ The Warburg effect in tumor cells increases glycolysis about 200-fold when compared to normal cells. Under the Warburg effect, the majority of glucose carbon is converted to lactate for excretion and cannot be used in the mitochondrial tricarboxylic acid (TCA) cycle.² To make for this loss, cancer cells develop unusual glutamine dependence.³ Glutamine is an essential nutrient for cancer cells, and is hydrolyzed to glutamate and ammonia by glutaminases and amidohydrolase enzymes. Therefore, glutaminases are overexpressed in many cancer cells.⁴

There are two isoforms of glutaminase in mammalian tissues.⁵ They are located on distinct chromosomes but structurally related genes. Kidney-type glutaminase (GLS1) is widely found in extra hepatic tissues, whereas liver-type glutaminase (GLS2) exists primarily in the adult liver. GLS1 is overexpressed in many primary tumors, whereas GLS2 is not. To this end, treatment with an efficient GLS1 inhibitor in different tumor models or genetic silencing of GLS1 has been validated as a therapeutic cancer target.⁶

Various GLS inhibitors have been reported as anticancer agents, and they can be categorized as *orthosteric inhibitors* (active site inhibition) and *allosteric inhibitors* (other than active site inhibition) as shown in Fig. 1. The *orthosteric inhibitors* such as acivicin and 6-diazo-5-oxo-L-norleucine (DON) bind covalently to the active site of GLS and other

* Corresponding authors at: Bio & Drug Discovery Division, Korea Research Institute of Chemical Technology, Daejeon 34114, South Korea (K. Lee).

E-mail addresses: CBC1971@yuhs.ac (B.C. Cho), kwangho@krikt.re.kr (K. Lee).

¹ E.J.L., K.B.D., Y.L. and M.R.Y. contributed equally to this work.

enzymes, and show modest anticancer activity but have high toxicity, perhaps due to the lack of selectivity against glutamate dehydrogenase, γ -glutamyl transpeptidase, and others which recognize glutamine or glutamate as substrates.⁷ On the contrary, the *allosteric inhibitor*, featured with bis-2-[5-(phenylacetamido)-1,3,4-thiadiazol-2-yl]ethyl sulfide (BPTES), has a novel mode of inhibition and an astounding selectivity toward GLS1 over GLS2.⁸

GLS exists as either an inactive dimer or an active tetramer.⁵ When inactive GLS dimers dimerize into a symmetric tetramer, the tetramer shows glutaminolysis catalytic activity. The interface of two GLS dimers would be structurally symmetrical, and thus the symmetrical BPTES uniquely binds between the lipophilic dimer interfaces of two GLS subunits occupying equivalent spaces on each protein.⁹ BPTES offers several advantages over conventional catalytic site inhibitors such as DON and acivicin. First, BPTES is an allosteric inhibitor, and does not have structural similarity to either glutamine or glutamate. Therefore, BPTES could minimize toxicological risk due to its interaction with other enzymes, transporters, or receptors that recognize glutamine or glutamate as substrates. In addition, BPTES selectively inhibits GLS1 over GLS2 and γ -glutamyl transpeptidase via a unique inactive tetramer formation: the GLS1 active site forms a closed conformation with a stabilized Glu312-Pro329 loop. However, BPTES pulls this lipophilic Glu312-Pro329 loop 18 Å away from the active site and induces an open conformation, resulting in enzyme inactivation in an allosteric manner. This is why BPTES is a highly hydrophobic and symmetric molecule with very poor solubility (aqueous solubility less than 1 µg/mL).¹⁰ Its poor aqueous solubility results in suboptimal pharmacokinetic parameters and hinders its further development.¹¹ To this end, CB-839 and IACS-6274 were discovered as a result of optimization from BPTES, and are currently under clinical evaluation for multiple cancer treatment studies.¹² For their potential use of combination therapies with other anticancer agents, we believe there is room to improve their physicochemical and pharmacokinetic properties of current GLS1 inhibitors. Herein we wish to describe our effort to identify more drug-like GLS1 inhibitors via systematic *structure – activity relationship* (SAR) analysis of analogs derived from BPTES: to improve their pharmacokinetic properties, we designed macrocyclic inhibitors for increased plasma and microsomal stabilities. To increase aqueous solubility, we introduced more oxygen atoms into the wing linker. Xu *et al.* recently published their macrocyclic GLS1 inhibitors using olefin metastasis chemistry, but our approach is to put more oxygen atoms in the wing linker to improve

solubility, which is different from their report.¹³ Inspired from the X-ray co-crystal structure of GLS1 with BPTES and CB-839, we designed macrocycles with ethylene or propylene or alkylene ethers at the wing linkers as shown in Fig. 2.

With this medicinal chemistry strategy in hand, we launched a synthetic chemistry campaign as drawn in Scheme 1. 6-Chloropyridazin-3-amine was protected as di-*tert*-butylcarbonyl (Boc) chloropyridazin-3-amine **int-1**. The Sonogashira reaction with ethynyltrimethylsilane using palladium and copper(I) iodide converted **int-1** into silylated **int-2**. Methanolysis with potassium carbonate provided the de-silylated 6-ethynylpyridazin **int-3**. The dimerization of 6-ethynylpyridazin **int-3** was successfully accomplished using copper(I) chloride and pyridine under ambient air to give **int-4**. Careful hydrogenation of **int-4** using palladium hydroxide in tetrahydrofuran and *N,N*-dimethylformamide provided **int-5**, and subsequent hydrolysis using trifluoroacetic acid afforded the symmetric pyridazine amine **int-6**. Symmetric thiadiazole amine and asymmetric pyridazine-thiadiazole amine were prepared according to a previously reported procedure.¹⁴ Dipropylene glycol was di-tosylated with tosyl chloride and sodium hydroxide to provide **int-7**. **Int-7** was then coupled with *tert*-butyl 2-(3-hydroxyphenyl)acetate and cesium carbonate to afford di-*tert*-butyl ester **int-8**. Di-*tert*-butyl ester **int-8** was hydrolyzed using trifluoroacetic acid to give di-acid **int-9**. Di-acid **int-9** was converted into di-acid chloride using oxalyl chloride, followed by *in situ* addition of **int-6** with triethylamine to generate the desired symmetric macrocyclic compound **13**. All macrocycles, **1–15**, were prepared through this chemistry route.

First, to survey the macrocycle core linker length effect, *n*-propylene (**1**), *n*-butylene (**2**), and *n*-pentylene (**3**) core linker analogs were prepared, and their GLS1 biochemical activities were measured (Table 1). Consistent as the previous report, the *n*-butylene molecule (**2**) is most active, followed by *n*-propylene (**1**) and *n*-pentylene (**3**) analogs in this study.¹⁴ From this SAR result, we select the *n*-butylene as default core linker on our macrocyclic molecule study.

Next, we examined the effect of the number of ethylene glycols in the wing linker (Table 2). Mono-ethylene glycol (**5**), di-ethylene glycol (**2**), tri-ethylene glycol (**6**) and tetra-ethylene glycol (**7**) derivatives were prepared along with their acyclic parent molecule (**4**). Undoubtedly, acyclic (**4**) molecule was almost inactive in our assay (GLS1 IC₅₀ > 10 µM), and all the cyclic derivatives showed a level of potency toward GLS1. The smaller the number of wing linker atoms of the macrocyclic inhibitor, the more potent to the GLS1: mono-ethylene glycol (**5**) is most

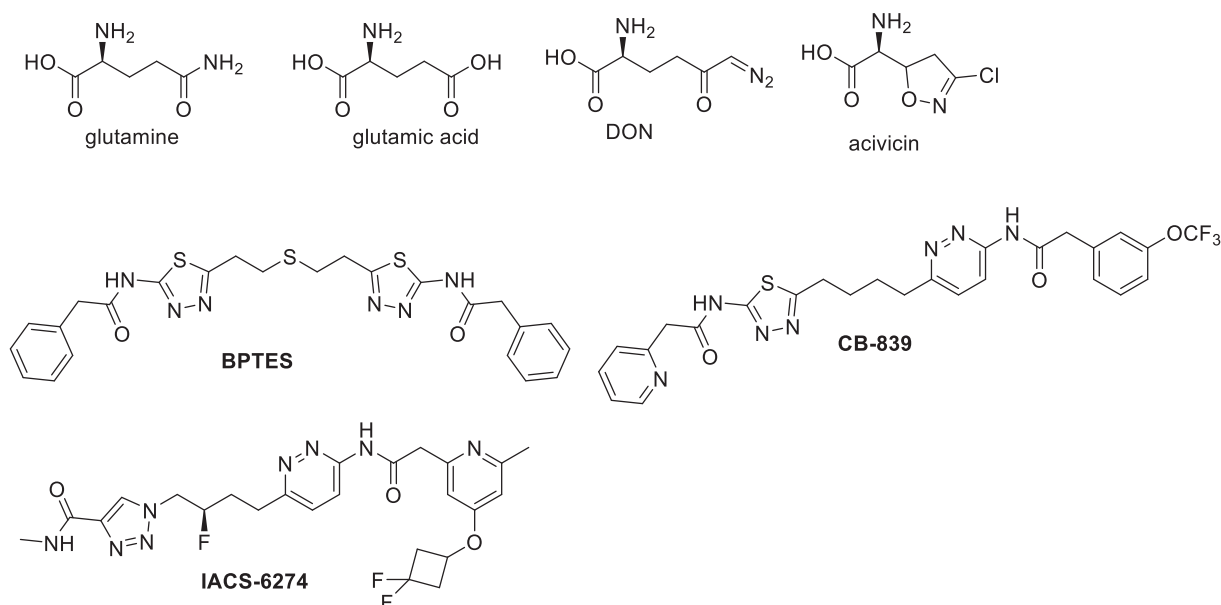


Fig. 1. Glutaminase inhibitors.

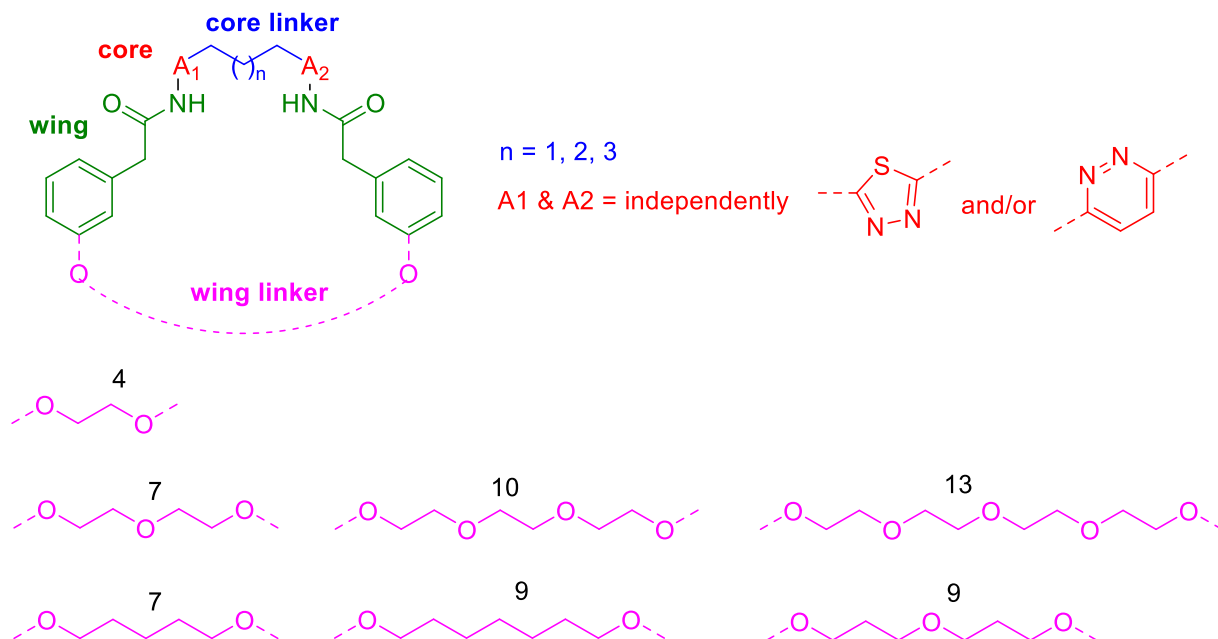
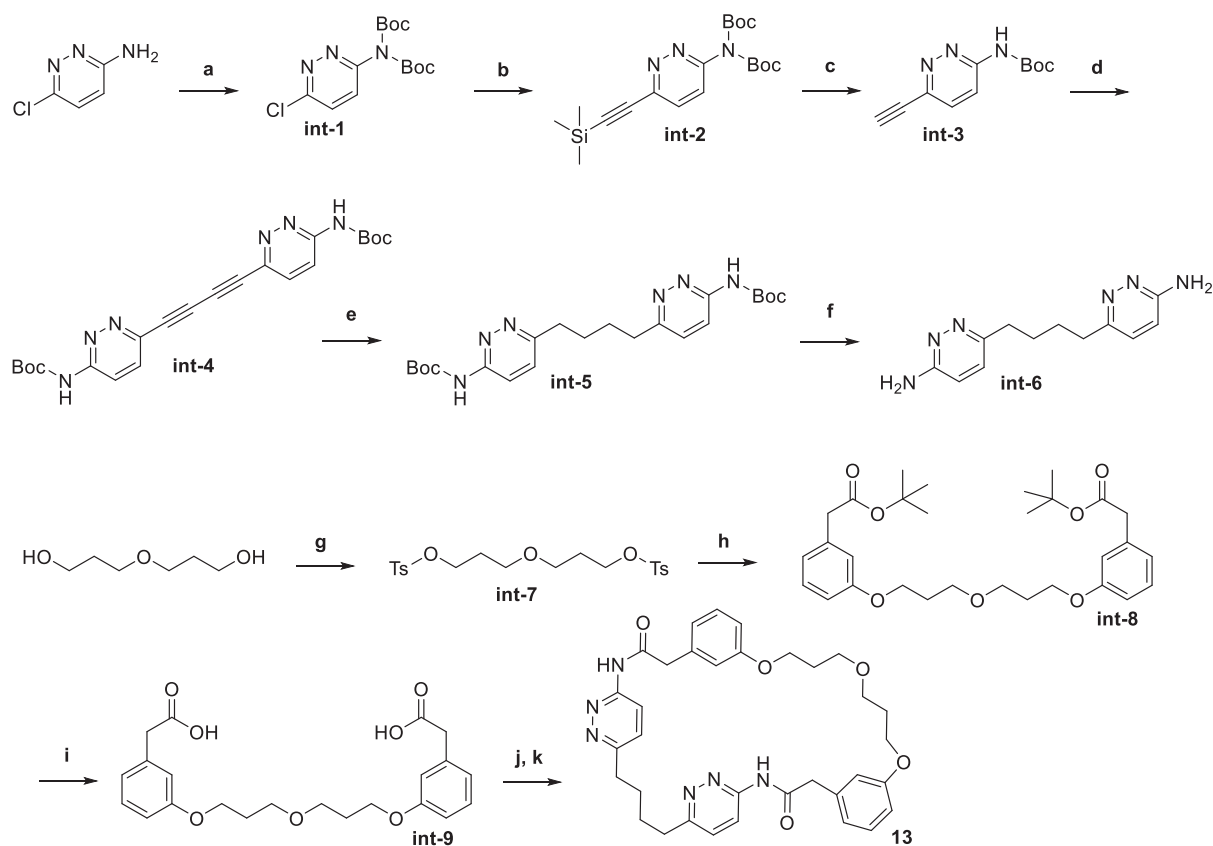


Fig. 2. Medicinal chemistry strategy for macrocyclic GLS1 inhibitor.



Scheme 1. Reagents and conditions: (a) Boc_2O , TEA, DMAP, DCM, rt, o/n (63 %); (b) $\text{PdCl}_2(\text{PPh}_3)_2$, CuI, ethynyltrimethylsilane, TEA, THF, 50 °C, o/n (79 %); (c) K_2CO_3 , MeOH, rt, 1 h (quantitative); (d) CuCl, pyridine, air, rt, 1 h (quantitative); (e) $\text{Pd}(\text{OH})_2$, H_2 , THF/DMF, rt, o/n (56 %); (f) TFA, rt, 2 h (quantitative); (g) TsCl, NaOH, DCM, rt, o/n (94 %); (h) *tert*-butyl 2-(3-hydroxyphenyl)acetate, NaI, Cs_2CO_3 , DMSO, 90 °C, o/n (56 %), (i) 30 % TFA in DCM, rt, 1 h (quantitative); (j) $(\text{COCl})_2$, DMF (cat.), toluene, rt, 1 h; (k) int-6, TEA, DMF, rt, o/n (24 % in two steps).

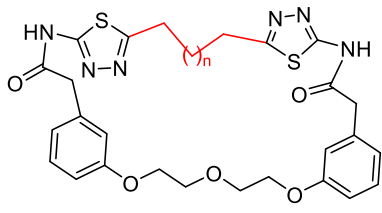
potent, followed by di-ethylene glycol (2), tri-ethylene glycol (6) and tetra-ethylene glycol (7) derivatives in this series.

We then investigated the core SAR study as summarized in Table 3.

Symmetric bis-thiadiazole (2) and bis-pyridazine (8) analogs and asymmetric thiadiazole-pyridazine molecule (9) were synthesized, and their GLS1 potency was compared. Symmetric bis-thiadiazole (2) was

Table 1

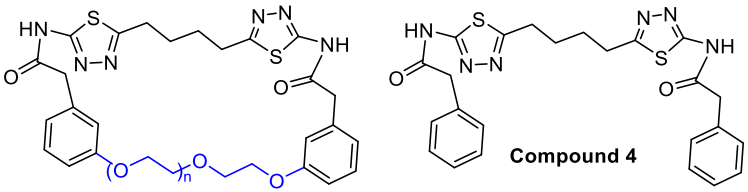
Biochemical activities by regulating number of carbons on the core linker.



Compound	# of carbon on core linker	# of core thiadiazole	# of core pyridazine	# of oxygen atoms on wing linker	# of atoms on wing linker	GLS1 IC ₅₀ (μM)
CB-839						0.2
1	3 (n = 1)	2	0	3	7	4
2	4 (n = 2)	2	0	3	7	2
3	5 (n = 3)	2	0	3	7	10

Table 2

Biochemical activities by regulating number of oxygens and total atoms on the wing linker.



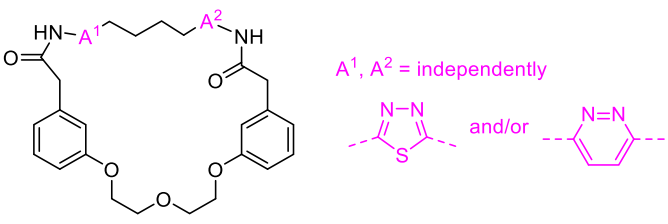
Compound	# of carbon on core linker	# of core thiadiazole	# of core pyridazine	# of oxygen atoms on wing linker	# of atoms on wing linker	GLS1 IC ₅₀ (μM)
CB-839						0.2
4	4	2	0			>10
5	4	2	0	2	4	0.98
2	4	2	0	3	7	2
6	4	2	0	4	10	3
7	4	2	0	5	13	4

the least potent in this comparison, and both bis-pyridazine (8) and asymmetric thiadiazole-pyridazine (9) were equally potent for GLS1 inhibition in this study.

Finally, we examined the effect of oxygen on the wing linker. As shown in Table 4, compound 10 has *n*-pentylene diol in the wing linker whereas compound 9 has di-ethylene glycol in the wing linker:

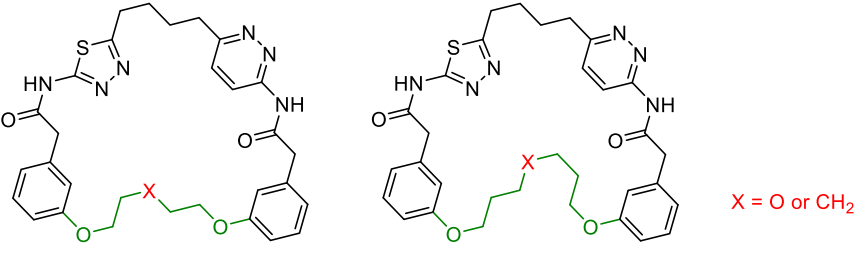
compound 9 is more potent than compound 10 toward GLS1 inhibition. Other examples are the compounds 11 and 12. Compound 11 has *n*-heptylene diol in the wing linker, whereas compound 12 has di-propylene glycol in the wing linker: compound 12 is more potent than compound 11 to GLS1. It is noteworthy to mention that the smaller size of the wing linker molecules (10, 9) are more potent than their larger

Table 3
Biochemical activities by regulating the heteroaromatic cores.



Compound	# of carbon on core linker	# of core thiadiazole	# of core pyridazine	# of oxygen atoms on wing linker	# of atoms on wing linker	GLS1 IC ₅₀ (μM)
CB-839						0.2
2	4	2	0	3	7	2
8	4	0	2	3	7	0.43
9	4	1	1	3	7	0.4

Table 4
Biochemical activities by regulating number of oxygens and total atoms on the wing linker.



Compound	# of carbon on core linker	# of core thiadiazole	# of core pyridazine	# of oxygen atoms on wing linker	# of atoms on wing linker	GLS1 IC ₅₀ (μM)
CB-839						0.2
10	4	1	1	2	7	1
9	4	1	1	3	7	0.4
11	4	1	1	2	9	3
12	4	1	1	3	9	0.8

homologs (11, 12) in this series as well (*vide supra*). Based on the above results, we conclude that additional oxygen atoms in the wing linker may boost GLS1 potency.

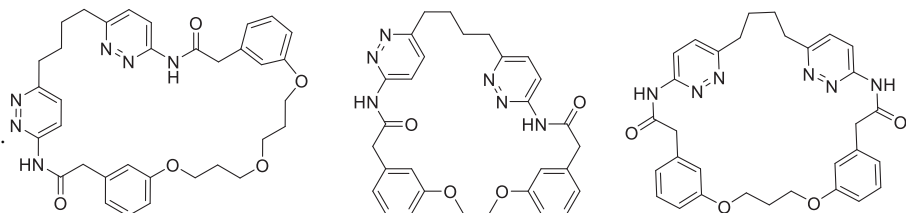
To this end, we could identify a series of potent macrocyclic molecules for GLS1 inhibition after an intensive SAR study: compounds 13, 14, and 15 are most potent to GLS1 inhibitors in this medicinal campaign (GLS1 IC₅₀ = 0.18–0.31 μM) which are comparable to CB-839

(GLS1 IC₅₀ = 0.2 μM), as summarized in Table 5.

The selected compounds (8, 9, 13, 14, and 15) were further evaluated using a cellular assay. Previous preclinical studies reported that alterations in the KEAP1/NRF2 pathway drives metabolic adaptations in tumor cells, and that results in glutamine dependence and vulnerability to glutaminase inhibition.¹⁵ Based on these reports, we evaluated the effect of pharmacologic glutaminase inhibition of selected compounds

Table 5

Novel and potent macrocyclic GLS1 inhibitors.



Compound	# of carbon on core linker	# of core thiadiazole	# of core pyridazine	# of oxygen atoms on wing linker	# of atoms on wing linker	GLS1 IC ₅₀ (μM)
CB-839						0.2
13	4	0	2	3	9	0.31
14	4	0	2	2	4	0.18
15	4	0	2	2	5	0.18

compared to CB-839 in glutamine-addicted LR (LDK378-resistant) cells. Although all compounds dose-dependently inhibited LR cell growth, CB-839 and compound 13 exhibited more potent anti-proliferative effects than tested other compounds with IC₅₀ values of less than 0.1 μM (Fig. 3A). The discrepancy between GLS1 biochemical and LR cellular activities may be due to differences in cell permeability between the tested molecules.

As part of the mechanism of action study, intracellular glutamate/glutamine levels were evaluated with selected molecules. Consistent with cell viability results, all compounds resulted in significant reduction in intracellular glutamate levels in LR cells at a concentration of 0.3 μM, of which CB-839 and compound 13 were most effective (Fig. 3B). It is important to mention that a high intracellular glutamine concentration was maintained in all the tested compounds. We further confirmed the potency of compound 13 in KRAS-mutant lung adenocarcinomas with KEAP1 mutations. As expected, CB-839 and compound 13 dramatically reduced the growth of A549 and H460 cells, which have co-occurring mutations including KRAS and KEAP1, but had little effect on H358 cells that harbor only KRAS mutations (Fig. 4). Taken together, these results suggest that both CB-839 and compound 13 exert antitumor

effects on glutamine-addicted tumor cells by effectively inhibiting glutaminase.

We attempted to explain GLS1 inhibition by compound 13 using a molecular modeling study, as depicted in Fig. 5. Like CB-839, compound 13 occupies the allosteric pocket of the solvent-exposed region between the activation loops of the homo-dimeric proteins. The chemical structure of compound 13 has internal symmetry, with two exactly equivalent parts, including a pyridazine, amide, and a phenyl group, and it equally interacts with each monomer chain. The activity of compound 13 was ascribed mainly to several strong hydrogen bonds and hydrophobic interactions. The pyridazine ring and amide N formed strong hydrogen bonds with the mainchain N of Phe322 and Leu323, and O of Leu323. The amide bond O also formed a hydrogen bond with the NZ of Lys320. The pyridazine groups and aliphatic linker were well-stabilized in the hydrophobic pocket consisting of Leu321, Phe322, Leu323, and Tyr394 from both monomers. Additionally, the cation-π interaction of the phenyl group with the NH1 of Arg317 also contributes to binding stability.

In conclusion, starting with the GLS1 allosteric inhibitor BPTES, which has poor solubility and pharmacokinetic properties, we designed

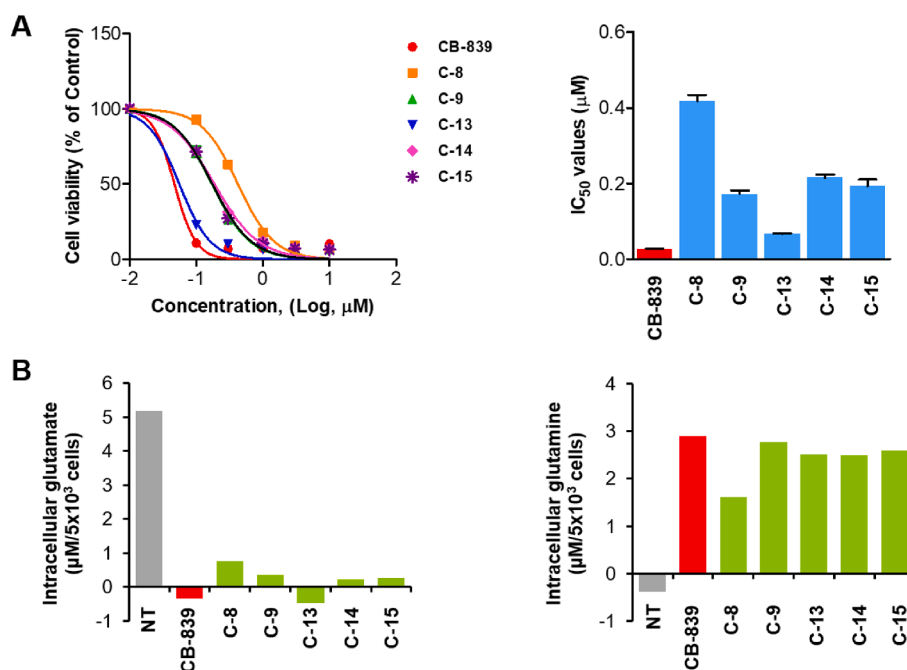
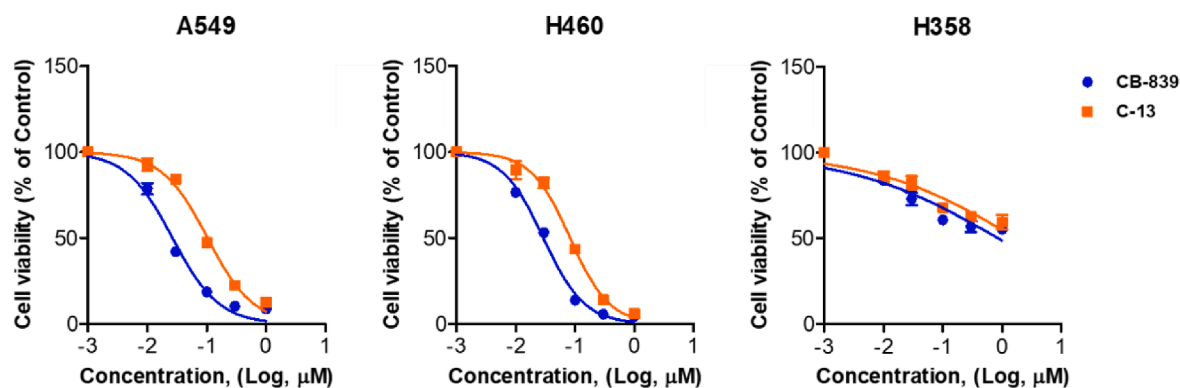


Fig. 3. A, Dose-response curves of cell viability by Cell Titer-Glo of LR cells treated with 0, 0.01, 0.03, 0.1, 0.3, 1 μM of the indicated compounds for 72 h (left) and IC₅₀ values of each compounds (right). B, Intracellular glutamate levels (left) and intracellular glutamine levels (right) in LR cells at 24 h after treatment with the indicated compounds at a 0.3 μM concentration.



Cell lines	Genetic alteration	IC ₅₀ , μM	
		CB-839	compounds 13
A549	KRAS (G12S), STK11 (Q37*), KEAP1 (G333C)	0.026	0.095
H460	KRAS (Q61H), PIK3CA (E545K), STK11 (Q37*), KEAP1 (D236H)	0.036	0.088
H358	KRAS (G12C), P53 null	>1	>1

Fig. 4. Dose–response curves of cell viability by Cell Titer-Glo of indicated cells after treatment with 0, 0.01, 0.03, 0.1, 0.3, 1 μM of CB-839 and C-13 for 72 h (upper) and IC₅₀ values of each compound (bottom).

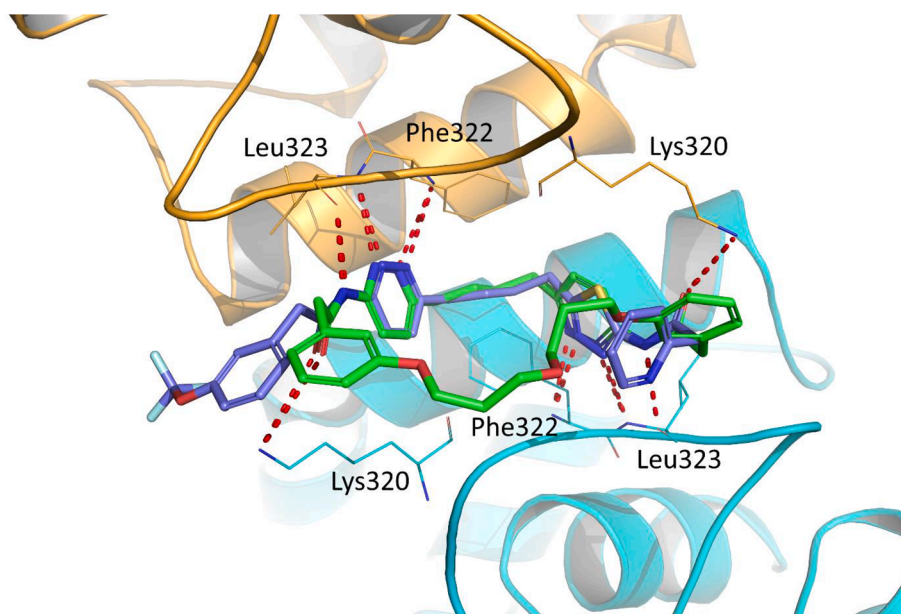


Fig. 5. Proposed binding pose of compound 13 (green) in the allosteric site of glutaminase (PDB ID: 5HL1) complexed with CB-839 (blue). Glutaminase chains are depicted in ribbons (A-chain: cyan; B-chain: orange), and only hydrogen-bonding interaction (red dots) residues are displayed in thin sticks for clarity. (For interpretation of the references to colour in this figure legend, the reader is referred to the web version of this article.)

macroyclic inhibitors with additional oxygen atoms in the wing linker to improve plasma and microsomal stability and increase aqueous solubility. The synthetic chemistry of macrocyclic compound 13 is described, and the SAR study of the macrocycles toward GLS1 is carefully disclosed on the core, core linker, and wing linker. Compound 13 was identified as a potent macrocyclic GLS1 inhibitor in both biochemical and cell viability assays. Compound 13 resulted in the greatest reduction in intracellular glutamate levels in LR cells, which was consistent with the cell viability results. In addition, compound 13 selectively reduced the growth of A549 and H460 cells, which have co-

occurring mutations including KRAS and KEAP1. The putative binding mode of compound 13 was also described using a molecular docking model. Further lead optimization of compound 13 is currently underway and will be reported in due time.

Declaration of Competing Interest

The authors declare that they have no known competing financial interests or personal relationships that could have appeared to influence the work reported in this paper.

Data availability

No data was used for the research described in the article.

Acknowledgments

This research was supported by Korea Drug Development Fund funded by Ministry of Science and ICT, Ministry of Trade, Industry, and Energy, and Ministry of Health and Welfare [HN21C1180], National Research Foundation of Korea grant [No. 2022R1A2C3005817], and Korea Research Institute of Chemical Technology [KK2231-20]. Authors thank Editage (www.editage.co.kr) for English language editing.

Appendix A. Supplementary data

Supplementary data to this article can be found online at <https://doi.org/10.1016/j.bmcl.2022.128956>.

References

- Warburg O. On the origin of cancer cells. *Science*. 1956;123:309–314. <https://doi.org/10.1126/science.123.3191.309>.
- Hensley CT, Wasti AT, DeBerardinis RJ. Glutamine and cancer: cell biology, physiology, and clinical opportunities. *J Clin Invest*. 2013;123:3678–3684. <https://doi.org/10.1172/JCI69600>.
- (a) Rubin AL. Suppression of transformation by and growth adaptation to low concentrations of glutamine in NIH-3T3 cells. *Cancer Res*. 1990; 50; 2832–2839; (b) Yuneva M, Zamboni N, Oefner P, Sachidanandam R, Y. Lazebnik Y. Deficiency in glutamine but not glucose induces MYC-dependent apoptosis in human cells. *J. Cell Biol*. 2007; 178; 93–105. 10.1083/jcb.200703099.
- (a) Ru P, Williams TM, Chakravarti A, Guo D. Tumor metabolism of malignant gliomas. *Cancers*. 2013; 5; 1469–1484. 10.3390/cancers5041469; (b) Tanaka K, Sasayama T, Irino Y, et al. Compensatory glutamine metabolism promotes glioblastoma resistance to mTOR inhibitor treatment. *J Clin Invest*. 2015; 125; 1591–1602. 10.1172/JCI78239.
- Curthoys NP, Watford M. Regulation of glutaminase activity and glutamine metabolism. *Annu Rev Nutr*. 1995;15:133–159. <https://doi.org/10.1146/annurev.nu.15.070195.001025>.
- (a) Chen SS, Yu KK, Ling QX, et al. *Sci Rep*. 2016; 6; No. 24582; (b) Cassago A, Ferreira APS, Ferreira IM, et al. Mitochondrial localization and structure-based phosphate activation mechanism of Glutaminase C with implications for cancer metabolism. *Proc Natl Acad Sci USA*. 2012; 109; 1092–1097. 10.1073/pnas.1112495109.
- Shapiro RA, Clark VM, Curthoys NP. Inactivation of rat renal phosphate-dependent glutaminase with 6-diazo-5-oxo-L-norleucine. Evidence for interaction at the glutamine binding site. *J Biol Chem*. 1979;254:2835–2838. [https://doi.org/10.1016/S0021-9258\(17\)30149-7](https://doi.org/10.1016/S0021-9258(17)30149-7).
- Robinson MM, McBryant SJ, Tsukamoto T, et al. Novel mechanism of inhibition of rat kidney-type glutaminase by bis-2-(5-phenylacetamido-1,2,4-thiadiazol-2-yl)ethyl sulfide (BPTES). *Biochem J*. 2007;406:407–414. <https://doi.org/10.1042/BJ20070039>.
- Thangavelu K, Pan CQ, Karlberg T, et al. Structural basis for the allosteric inhibitory mechanism of human kidney-type glutaminase (KGA) and its regulation by Raf-Mek-Erk signaling in cancer cell metabolism. *Proc Natl Acad Sci U S A*. 2012;109: 7705–7710. <https://doi.org/10.1073/pnas.1116573109>.
- Shukla K, Ferraris DV, Thomas AG, et al. Design, synthesis, and pharmacological evaluation of bis-2-(5-phenylacetamido-1,2,4-thiadiazol-2-yl)ethyl sulfide 3 (BPTES) analogs as glutaminase inhibitors. *J Med Chem*. 2012;55:10551–10563. <https://doi.org/10.1021/jm301191p>.
- (a) Chen Z, Li D, Xu N, et al. Novel 1,3,4-Selenadiazole-Containing Kidney-Type Glutaminase Inhibitors Showed Improved Cellular Uptake and Antitumor Activity. *J Med Chem*. 2019; 62; 589–603. doi: 10.1021/acs.jmedchem.8b01198; (b) Soth MJ, Le K, Francesco MED, et al. Discovery of IPN60090, a Clinical Stage Selective Glutaminase-1 (GLS-1) Inhibitor with Excellent Pharmacokinetic and Physicochemical Properties. *J Med Chem*. 2020; 63; 12957–02977. 10.1021/acs.jmedchem.0c01398; (c) Zimmermann SC, Duvall B, Tsukamoto T. Recent Progress in the Discovery of Allosteric Inhibitors of Kidney-Type Glutaminase. *J Med Chem*. 2019; 62; 46–59. 10.1021/acs.jmedchem.8b00327; (d) Finlay MRV, Anderton M, Bailey A, et al. Discovery of a Thiadiazole–Pyridazine-Based Allosteric Glutaminase 1 Inhibitor Series That Demonstrates Oral Bioavailability and Activity in Tumor Xenograft Models, *J Med Chem*. 2019; 62; 6540–6560. 10.1021/acs.jmedchem.9b00260.
- Meric-Bernstam F, Lee RJ, et al. CB-839, a glutaminase inhibitor, in combination with cabozantinib in patients with clear cell and papillary metastatic renal cell cancer (mRCC): results of a phase I study. *J Clin Oncol*. 2019;37:549. https://doi.org/10.1200/JCO.2019.37.7_suppl.549.
- Xu X, Wang J, Wang M, et al. Structure-enabled discovery of novel macrocyclic inhibitors targeting glutaminase 1 allosteric binding site. *J Med Chem*. 2021;64: 4588–4611. <https://doi.org/10.1021/acs.jmedchem.0c02044>.
- WO 2013/078123; WO 2016/022969.
- (a) Binkley MS, Jeon YJ, Nesselbush M, et al. KEAP1/NFE2L2 Mutations predict lung cancer radiation resistance that can be targeted by glutaminase inhibition. *Cancer Discov*. 2020; 10; 1826–1841. 10.1158/2159-8290.CD-20-0282; (b) Romero R, Sayin VI, Davidson SM, et al. Keap1 loss promotes Kras-driven lung cancer and results in dependence on glutaminolysis. *Nat Med*. 2017; 23; 1362–1368. 10.1038/nm.4407.